MONITORING FOREST DYNAMICS IN NORTHEASTERN CHINA
IN SUPPORT OF GOFC

Progress Report
May 1, 2001 – April 30, 2002

by

Guoqing Sun
Department of Geography, University of Maryland, College Park, MD 20742
Phone: 301-614-6655, Fax: 301-614-6695, ENAIL: guoqing@taiga.gsfc.nasa.gov

D. L. Williams
Biospheric Sciences Branch - Code 923, Goddard Space Flight Center, Greenbelt, MD 20771
Phone: 301-614-6692, E-mail: darrel.williams@gsfc.nasa.gov

J. Masek
Biospheric Sciences Branch - Code 923, Goddard Space Flight Center, Greenbelt, MD 20771
Phone: 301-614-6629, E-mail: jmasek@ltpmail.gsfc.nasa.gov

K. J. Ranson
Biospheric Sciences Branch - Code 923, Goddard Space Flight Center, Greenbelt, MD 20771
Phone: 301-614-6650, E-mail: jon@taiga.gsfc.nasa.gov

April 24, 2002

ABSTRACT

During the second year of this project we have:

1) conducted field work in China in collaboration with our Chinese Co-I's;

2) acquired MODIS 16-day composite data available from June 2000 to October 2001. After these data were re-projected into Lambert Conformal Conic projection and mosaiced for the study area, the temporal data were classified using several methods (Maximum Likelihood, Oblique Decision Tree, and Isodata). The results were preliminary evaluated against ground-based observations and other land-cover products.

3) acquired orthorectified landsat-5 TM (centered on the 1990 epoch) and Landsat 7 ETM+ (1999-2001) images covering the mountainous perimeter of NE China and Eastern Mongolia, and have begun work on a detection algorithm for assessing both deforestation and reforestation in NE China during the last 10-20 years.

4) investigated the forest recovery from fire using Landsat-5 TM, Landsat-7 ETM+, ERS-1/2 SAR and JERS-1 SAR data. The capabilities of Landsat-7 ETM+ and SAR data for distinguishing between forests with different leaf longevity, canopy cover and height, and timber volume were preliminarily tested.

Our work in the third year of the project will include:

1) completing a validated 500m land (forest) cover map from temporal MODIS data;

2) establishing a baseline for assessing both deforestation and reforestation in NE China during the last 10-20 years from Landsat 5 and 7 data, and comparing these satellite-based estimates with other published estimates.

3) investigating the capabilities of new data (ENVISAT ASAR) for deriving forest physical parameters;

4) quantifying the impact of forest cover changes in the region during the last two decades on the carbon cycle using historical and updated forest cover maps, and

5) performing test runs to predict forest dynamics using this database and selected forest growth models useful for forest management strategies and assessments of carbon dynamics.

Key Words: 1) Research Fields: Forest Dynamics, GOFC, Change Detection, Carbon; 2) Geographic Area/Biome: Northern China, Boreal Forest, Temperate Forest; 3) Remote Sensing: Landsat, MODIS, SAR; 4) Methods/Scales: Land-cover Classification, Biomass Estimation, Regional

QUESTIONS, GOALS, AND APPROACHES

This project will try to answer the following questions:
- What are the changes in forest cover in NE China during the last two decades?
- What is the impact of these changes on forest carbon storage in this region?
- What are the causes of the forest cover changes in this region?

The proportion of social science to be used in this project is small – only in the later stage for the last question.

The goals for the second year were:

- Data collection: Acquire entire coverage of Landsat-7 ETM+ data for this region; Collect MODIS data and SAR data;

- Map forest type from MODIS, ETM+ and SAR data;

- Develop and test algorithms for biomass estimation using SAR and ETM+ data;

- Forest change detection from Landsat data;

- Field trip to test sites, develop sampling data for map validation;

- Attend LCLUC ST meeting, and send summary material and significant results to LCLUC Web Site

PROBLEMS:

- The planned acquisition of Landsat-7 data for the second year (30 scenes) has not been realized. The Landsat-7 data currently available to us doesn't cover the whole study area.

- EDC only acquires seasonal Landsat-7 coverage of our study area in China, which limits the possibility to get images with high-quality and similar acquisition dates for the region.

.

FIELD WORK CONDUCTED IN SUMMER 2001

A) Changbai Mountain and Lushuihe Forest Bureau:
- 10 persons (from US, Chinese Academy of Forestry, Nanjing University, Beijing Normal University, Local Forest Bureau)
- Worked for 9 days
- Total 28 stands were sampled for dbh, height, crown shape, stem density, and species composition, LAI
- Near 100 stands were observed in terms of forest type and structure.
- GPS and photos were taken for every stand.

B) Daxianling Forest:

- Five persons (from US, Chinese Academy of Forestry, Nanjing University, Northeastern Forestry University, and local Forest Bureau)
- Worked for a week
- Sampled birch regeneration and larch plantation after fire, unburned Larch and Scotch Pine stands. More than 50 stands were visited in an area of 50 km by 200 km.
- GPS and photos were taken for every stand.
- 1:50000 forest maps and survey data from several forest stations were acquired

PROGRESS IN RESEARCH

1) Forest and Land-use Mapping From Temporal MODIS Data

During the first year, we pursued forest-cover classification strategies using both MODIS and Landsat data. At the start of the second year, it was decided to use multitemporal MODIS data as the primary data source for the forest-cover assessments, and use Landsat data for forest-cover change estimates. As noted below, both Landsat and IKONOS imagery are used to supplement MODIS and provide training data for the classification tasks.

The MODIS 16-day 500m composite data (MOD13A) in Northeastern China (38° – 53° N, 115° – 135^oE) were used to map land cover with special attention to forest type. All available data from June 2000 to October 2001 were requested and re-projected from MODLAND Integerized Sinusoidal 10-degree Grid to Lambert Conformal Conic projection, and mosaicked (7 tiles). Various combinations of the data (e.g. time-series of NDVI, EVI, multi-band reflectance data) and different classification methods (e.g. clustering, MLC, decision-tree) were used and the results were evaluated and compared.

Forest maps (1:50000) and survey data collected in 1999 by the local Forest Management Bureau, IKONOS images, Landsat-7 ETM+ imagery and classification maps derived from the Landsat-7 data were used for training site location and map evaluation. For regional land-use characterization, the results demonstrate the advantages of the time-series MODIS data over single-date LANDSAT and SAR data.

Both supervised and unsupervised classification methods were tried to classify the 12 16-day NDVI composite data (starting days of 161, 257, 305, 321 of 2000 and 17, 65, 81, 97, 113, 145, 257, 273 of 2001). The study area was divided into several sub-regions (DX, EDX, XX, CB, etc.) based on the vegetation types and climate conditions and various classes were identified within each sub-region. A total 38 training sites were selected. Since the decision-tree classifier works better when the number of pixels of the training sites are similar, the pixels were randomly duplicated so that the number of the pixels in every training site was equal to the site with maximum number of pixels (i.e. Shrub-DX, 93 pixels).

Both methods gave very high overall accuracies (99.8% and 99.5%) for the training sites. However, the maps show obvious confusions. On MLC map, many bare, or

sparsely vegetated areas were confused with build-up areas, and the evergreen needle forests are overestimated. The ODT gives better results for these cases.

Figure 1 is a classification map using an unsupervised method – IsoData from ENVI. Originally, 255 clusters were generated. These clusters were than sorted according to the length and angle of mean vectors of these clusters. Then these clusters were assigned into general classes by use of the field observations, forest maps, Landsat data, IKONOS images. This map gives reasonable results in terms total forest coverage comparing to the Chinese statistics (Table 1).

During the coming summer, we will work with Chinese Collaborators to refine the training sites, try other bands (EVI, red, NIR, blue, MIR) and evaluate the classification methods using large-scale forest maps, and field observations to produce a final version of the forest (land) cover map of this region.
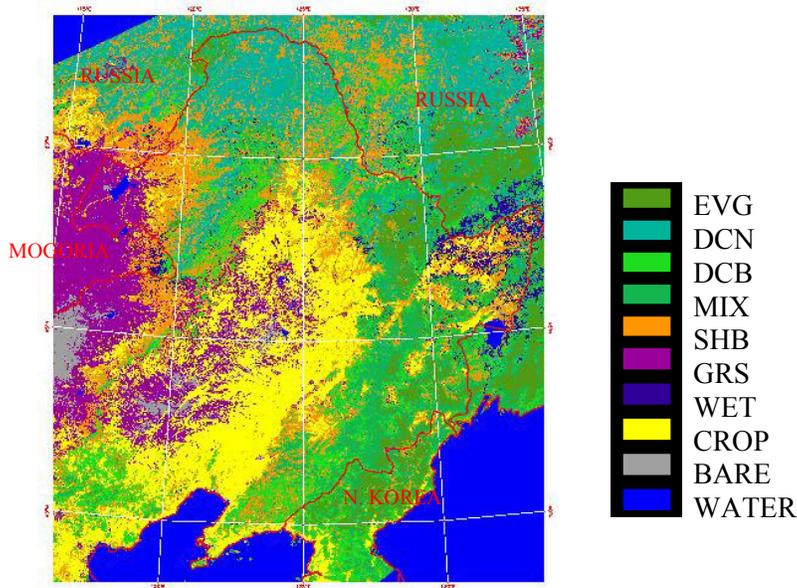

Figure 1. Classification map from unsupervised method.

Table 1. Percent forest cover by Province

	Ministry Forestry	Academy Forestry	MODIS 500m	MOD12 1km
Heilongjiang	34.4	41.9	48.8	50.8
Jilin	33.0	42.0	43.1	40.5
Liaoning	26.9	34.6	25.2	24.9

2) *Forest Cover Change in NE China 1990-2000*

Active harvesting of planted forests in Northeastern China, coupled with a vigorous program of reforestation, make the region a "hotspot" for assessing net balances in forest area, biomass, and carbon. Fang et al. (2001) reported significant increases in planted forests throughout NE China, leading to an overall increase of ~120,000 km2 in

Chinese forest cover since 1980. Our objectives for this part of the project are to establish a baseline for assessing both deforestation and reforestation in NE China during the last 10-20 years, compare these satellite-based estimates with other published estimates, and examine the biomass and carbon consequences of NE China forest dynamics.

The primary dataset used for our change detection work is the Landsat TM and ETM+ data archive. Some 64 ETM+ scenes have been acquired covering the mountainous perimeter of NE China and Eastern Mongolia. These data were orthorectified by USGS EDC, and converted to Lambert Conformal projection. Through the Science Data Purchase, we also acquired an equal number of orthorectified Landsat-5 TM scenes, centered on the 1990 epoch (actual dates 1987-1995). An initial assessment suggests that the two datasets cannot be automatically co-registered. Each was produced through a different orthorectification process (EDC vs. Earth Satellite Corporation) using different ground control libraries. As a result, geodetic errors of 2-3 pixels are observed when co-registering the data without further correction. To remedy this, we are applying an additional translation/rotation correction to each pair by picking ground control points, using the ETM+ as 'truth'. In addition, 18 of the Landsat-5 TM scenes were acquired either too early or too late in the growing season to permit comparison with the peak-greenness ETM+ data.

Our goal is to obtain an exact area of forest-cover change from Landsat, and use the MODIS land-cover products to establish the type of forests involved. This approach capitalizes on the fine spatial resolution and long archive of Landsat, as well as the excellent phonological (seasonal) characterization available from MODIS. From the Landsat data, we wish to obtain the following classes:

> *Mature Forest-to-nonforest*　　*(deforestation, urban expansion)*
> *Nonforest-to-mature forest*　　*(reforestation, fast recovery from disturbance)*
> *Mature Forest-to-regrowth*　　*(harvest cycles, slow recovery from disturbance)*
> *Regrowth-to-Mature Forest*　　*(completion of recovery cycle)*

Characterizing all four of these states will facilitate our estimates for forest-cover balance, and also yield a rough assessment of forest age structure, and key input for biomass calculations. Mapping the first two classes will be relatively straightforward; the second two more difficult.

The current change detection algorithm uses the Spectral Angle Mapper (SAM) concept, which is particularly robust in regions of variable illumination (eg. due to rough topography). Landsat data are first atmospherically corrected using a combination of dark-object subtraction and histogram matching, and converted to units of surface reflectance. Given two images at date 1 (t1) and date 2 (t2), the spectral vector may be defined as:

$V_1 = [r_13, r_14, r_15]$

and

$V_2 = [r_23, r_24, r_25]$

where (for example) r_13 refers to the reflectance of Landsat TM/ETM+ band 3 at t1. In the analysis we rely primarily on bands 3, 4,and 5 since these bands capture most of the

information content for vegetation, and are less susceptible to residual atmospheric effects than bands 1 and 2. The spectral change angle q may be defined as:

$$\theta = \cos^{-1}[(\mathbf{V_1} \bullet \mathbf{V_2}) / V_1 \, V_2]$$

where V_1 and V_2 refer to the magnitude of the two spectral vectors. Pixels that underwent significant change are mapped if θ exceeds a threshold established by training data. The type of change can then be determined by examining the endpoints of the spectral change vector supplemented with contextual information from the MODIS land-cover map. Since mature forest occupies a fairly well defined region of spectral space, we have established a series of thresholds in bands 3, 4, and 5 to demarcate the spectral "boundary" of mature forest. Change vectors crossing into this zone are considered to be reforestation, those crossing out are considered to be deforestation.

Preliminary results of the SAM change algorithm are presented below. Two reflectance images from the Changbai Mountain region are shown, acquired on May 28, 1993 (Fig. 2, upper left) and September 2, 1999 (upper right). The lower-left panel shows the spectral change angle θ (radians), while the lower-right panel shows the resulting deforestation (red) and regrowth (green) classes. Validation for these forest dynamics products relies on ground-truth estimates of forest age, biomass, height, and type provided by the Chinese Academy of Forestry, combined with visual interpretation of the imagery. During the next year we plan to validate the change-detection process for all of the regions of interest in the study, and finish the processing of all available Landsat data. The completed products will then be used as a basis for estimating decade-scale changes in forest biomass for the region.
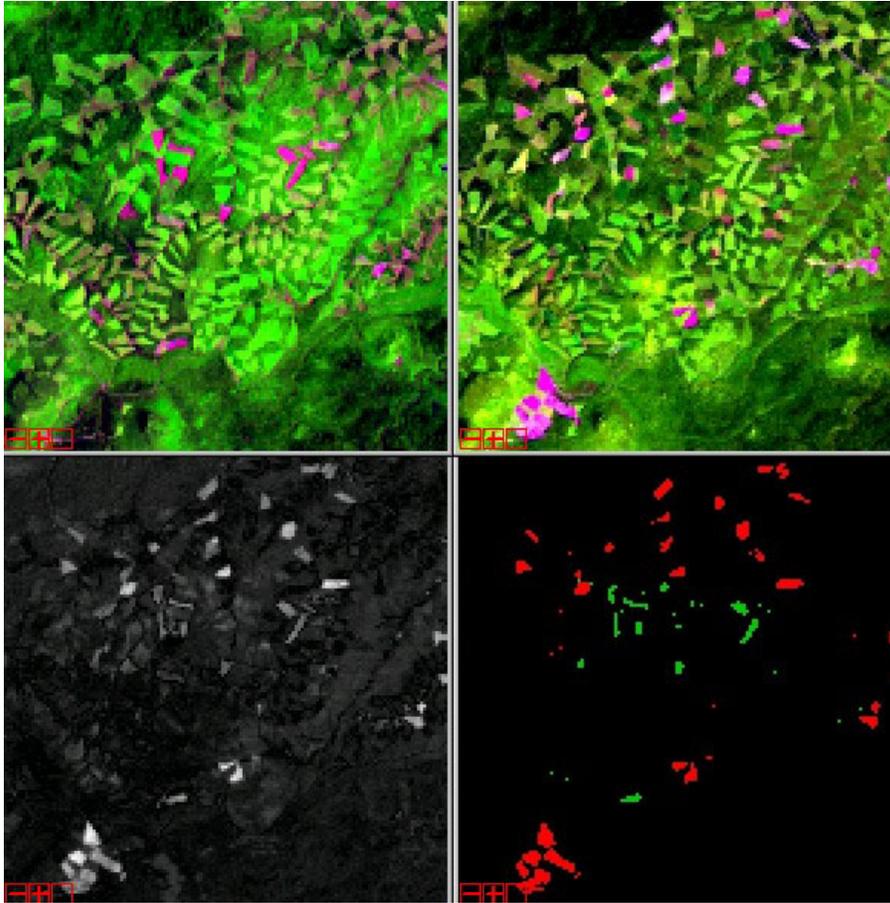
Figure 2. Two reflectance images from the Changbai Mountain region are shown, acquired on May 28, 1993 (upper left) and September 2, 1999 (upper right). The lower-left panel shows the spectral change angle θ (radians), while the lower-right panel shows the resulting deforestation (red) and regrowth (green) classes.

3) Characterization of Forest Recovery From Fire Using Landsat and SAR Data

A forest fire during May 6 – June 4, 1987 in Northeastern China burned 1.14 million hectares of forest (centered at 53°N/123°E) and nearly 25 million cubic meters of timber. The main forest species in this region are Dahurian Larch (*Larix gmelii*), Mongolian pine (*Pinus Sylvestris var mongolia*), and some broadleaf species, such as Asian White Birch (*Betula platyphylla*), David Poplar (*Populus davidiana*), Willows, Mongolian Oak (*Quercus mongolica*) and Dahurian Birch (*Betula dahurica*). About 70% of the forests were larch stands before the fire. The total biomass of mature larch forests in this area ranges from 10 to15 Kg/m^2.

The remote sensing data used in this study include Landsat-5 TM images from 12 June 1986, 15 June 1987, 11 October 1995, and 16 August 1998, processed by the Chinese Ground Station, a Landsat-7 ETM+ image from 10 June 2000 processed by Eros Data Center in the US, and JERS-1 L-band SAR data of 24-25 March 1997 from NASDA, Japan.

Forest survey data collected and mapped (1:50,000) in 1999 by the local Forest Management Bureau were registered to the 2000 Landsat-7 image. Additional field observations were conducted in summer 2001. Field samplings for biomass estimation and accompanying GPS locations were collected at various sites.
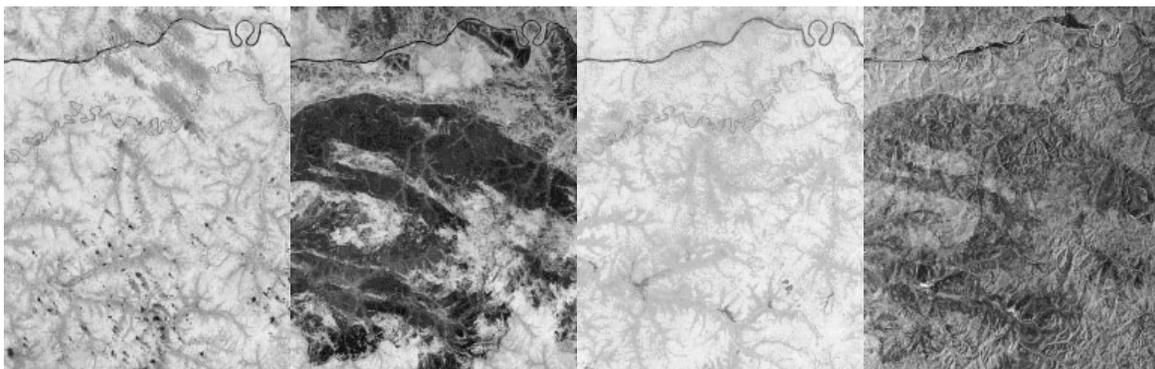
Remotely monitoring forest recovery requires consistent data, and consistency between sensors depends on validated radiometry. The radiometric calibration of the Landsat satellites allows quantitative time-series research to be conducted. Given the superior geometric integrity of Landsat-7, the 10 June 2000 data set served as the reference image to which the Landsat-5 data were registered. The image-to-image registration used nearest neighbor resampling and yielded a RMS < 1 pixel. Following image registration, a Dark Object Subtraction routine was used to normalize the varying atmospheric conditions by removing the effects of atmospheric path radiance.

For bands 3, 4, and 5 of each scene, the Landsat digital number (DN) was converted to top of atmosphere (TOA) radiance in $W/(m^2 \ sr \ \mu m)$ and subsequently to surface reflectance. This conversion is essential because the Landsat DN is an inappropriate index of change over time due to sensor calibration, solar zenith angle, sensor viewing angle, Earth-sun distance, and atmospheric factors that influence the DN value. Advantages of the DN-to-reflectance conversion are threefold; (1) removal of the cosine effect of varying solar zenith angles, (2) compensation for the range of exo-atmospheric solar irradiance between spectral bands, and (3) consistency between calculated TM and ETM+ NDVI results.

The Landsat-5 conversion from DN to radiance was calculated with the gains and biases provided in the data header. While these values are the best currently available, various studies have suggested that these coefficients may have changed slightly during the history of Landsat-5 operations. Landsat-7 conversion from DN to radiance took advantage of the LMIN and LMAX values provided on the *Landsat-7 Science Data Users Handbook* website. The most current exo-atmospheric solar irradiance values for both Landsat-5 and Landsat-7 were used in the radiance to reflectance conversion.

Using the reflectance values, both NDVI and a straight NIR/Red ratio were calculated, these served as our index for the photosynthetic recovery of the forest. Preliminary analysis suggests that the recovery trend is well documented by these indices. However, we have not yet accounted for the slightly different spectral range of the ETM+ sensor, which in previous studies has inflated ETM+ NDVI values ~2.5% on average.

Figure 3 shows four images: NDVI images of 1986 (a), after fire in 1987 (b) and 2000 (c), and the JERS-1 LHH image of 1997. The fire scar, which is very clear in the 1987 NDVI image, is not discernable on the 2000 image, indicating that in terms of vegetation greenness of LAI the vegetation cover is recovered. In fact, the fire scar is not visible in the 1995 NDVI image (not shown here). The L-band radar image from 1997 clearly shows the fire scar indicating that the woody structure or the total biomass of the forest has not yet recovered.

Figure 3. a – NDVI of June 12, 1986, b – NDVI of June 15, 1987, c – NDVI of June 10, 2000, d – JERS-1 SAR LHH of March 24-25, 1997.
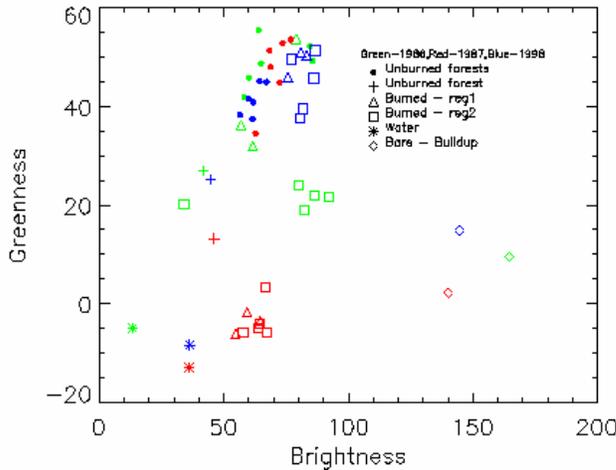
Figure 4. The forest recovery shown in Greenness-Brightness space. Colors represent date of the images: from green (1986), to red (1987) then to blue (1998). Symbols represent different targets.

The Tassled cap transform was used to assess changes in spectral behavior. Figure 4 shows the forest change in Greenness-Brightness. Unburned forests (dots) have consistently high greenness and relatively low brightness, as do dark forests (pluses). Forests severely burned in 1987 show similar recovery patterns despite differing 1986 greenness levels (squares represent lower initial greenness while triangles represent higher initial greenness). Water bodies (stars) and bare surfaces (diamonds) are dark and bright targets, respectively.

Another purpose of the study is to characterize current forests using Landsat and SAR data. The forest stands of three major species (larch, scotch pine and birch) with various ages were identified from forest maps, and the LHH backscattering from these stands were extracted. LHH backscattering was correlated with various forest parameters including age, average DBH, height, timber volume, crown closure, and logarithms of timber volume and DBH-square times height. Preliminary results show that the best correlation is between LHH backscattering and logarithm of DBH-square times height.

Similarly, the study using Landsat-7 data (NDVI and NIR/Red ratio) shows that the best correlation is between Landsat-7 data and crown closure. The simple NIR/Red ratio shows more texture or heterogeneity within forest stands which seem homogeneous in NDVI images. Our future work will focus on the relation between satellite signature and forest structure given the differing recovery processes.

COLLABORATIONS

9

1) With Dr. Sohn in UMBC on evaluation of classification methods in Changbai Mountain area
2) With Prof. Wayne Myerr in PSU on pattern-based and combinatorial change detection in burned area in Daxinganling. A 1986 pre-fire image serves as the base for pattern-comparative change vector images over several years using paired compressions by segmentation. In Fig. 5, CV8687 compares immediate pre-fire and post-fire conditions in 1986 and 1987. CV8698 compares 1986 and 1989 conditions, and likewise for CV8692 in 1992, and CV8699 in 1999. The image expression of fire scars (bright areas) has substantially faded in 1992.

| CV8687 | CV8689 | CV8692 | CV8699 |
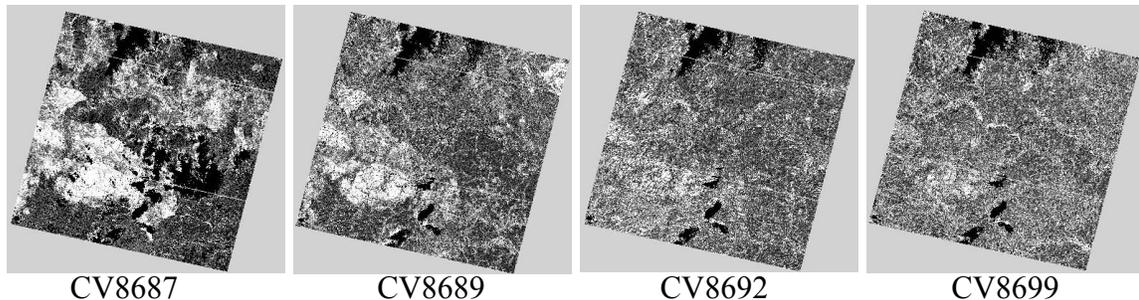
Figure 5. Forest fire and forest recovery from Landsat images using pattern-based and combinatorial change detection (Dr. W. Myers, The Pennsylvania State University).

PUBLICATIONS

Sun, G., et al., Forest Recovery from Fire Using Landsat and SAR Data, to be submitted to RSE in May, 2002.

Sun, G., et al., Land Cover Mapping From Temporal MODIS Data, to be submitted to RSE in June, 2002.

Sun, G., L. Rocchio, J. Masek, D. Williams, and K. Jon Ranson, Characterization of Forest Recovery From Fire Using Landsat and SAR Data, to be presented in IGARSS'02, June 24-28, 2002, Toronto, Canada.

Sun, G., D. Williams, J. Masek, and K. Jon Ranson, Characterization of Forest Recovery From Fire Using Landsat and SAR Data, to be presented in IGARSS'02, June 24-28, 2002, Toronto, Canada.

Sun, G., D. Williams, J. Masek, K. J. Ranson, and L. Rocchio, Monitoring forest dynamics in Northeastern China using multi-satellite data, Eos Trans. AGU, 82(47), Fall Meeting Suppl., San Francisco, USA 2001.

Sun, G., D. Williams, X. Zhan, Z. Li, J. Masek, K. J. Ranson, and L. Rocchio, Monitoring forest Dynamics using multi-sensor data in Northeastern China, IGARSS'01, 9-13 July 2001, university of New South Wales, Sydney, Australia.